Catalysis Today xxx (2012) xxx–xxx

Contents lists available at SciVerse ScienceDirect

Catalysis Today

journal homepage: www.elsevier.com/locate/cattod

Ti-functionalized NH_2-MIL-47: An effective and stable epoxidation catalyst

Karen Leus[a], Gauthier Vanhaelewyn[b], Thomas Bogaerts[a,c], Ying-Ya Liu[a], Dolores Esquivel[a], Freddy Callens[b], Guy B. Marin[d], Veronique Van Speybroeck[c], Henk Vrielinck[b,*], Pascal Van Der Voort[a,**]

[a] Department of Inorganic and Physical Chemistry, Center for Ordered Materials, Organometallics and Catalysis (COMOC), Ghent University, Krijgslaan 281-S3, 9000 Ghent, Belgium
[b] Department of Solid State Sciences, Ghent University, Electron Magnetic Resonance (EMR) Research Group, Krijgslaan 281-S1, 9000 Ghent, Belgium
[c] Center for Molecular Modeling, Ghent University, Technologiepark 903, 9052 Zwijnaarde, Belgium
[d] Laboratory for Chemical Technology, Ghent University, Krijgslaan 281-S5, 9000 Ghent, Belgium

ARTICLE INFO

Article history:
Received 13 July 2012
Received in revised form
14 September 2012
Accepted 18 September 2012
Available online xxx

Keywords:
Metal-organic frameworks
Vanadium
Titanium
Oxidation catalysis

ABSTRACT

In this paper, we describe the post-functionalization of a V-containing Metal-organic framework with $TiO(acac)_2$ to create a bimetallic oxidation catalyst. The catalytic performance of this V/Ti-MOF was examined for the oxidation of cyclohexene using molecular oxygen as oxidant in combination with cyclohexanecarboxaldehyde as co-oxidant. A significantly higher cyclohexene conversion was observed for the bimetallic catalyst compared to the non-functionalized material. Moreover, the catalyst could be recycled at least 3 times without loss of activity and stability. No detectable leaching of V or Ti was noted. Electron paramagnetic resonance measurements were performed to monitor the fraction of V-ions in the catalyst in the +IV valence state. A reduction of this fraction by ~17% after oxidation catalysis is observed, in agreement with the generally accepted mechanism for this type of reaction.

1. Introduction

Metal-organic frameworks (MOFs) are a highly versatile class of ordered porous materials constructed of metal nodes or metal clusters linked together by organic ligands. This recent class of crystalline materials has been extensively studied for their potential use in various applications, e.g. in gas storage and separations [1–3], catalysis [4–8] and luminescence [9,10]. MOFs possess many intriguing features including very high surface areas, well defined pore properties (pore size, shape and volume) and have easily tailorable structures and chemical functionalities. Several reports have appeared on the introduction of an additional functionality in the linker, by pre-functionalization with, e.g., $-NH_2$, $-OH$, $-CH_3$ and $-NO_2$ groups [11–15]. In the field of catalysis, it has been shown that the introduction of these additional functional groups can generate a significant alteration in the catalytic performance compared to the parent framework. In a recent report of Vermoortele et al., a UiO-66-X (X = H, NH_2, CH_3, OCH_3, F, Cl, Br, NO_2)series with different functional groups was tested for the citronellal cyclization [16]. This study demonstrated that the presence of $-NO_2$ groups enhanced the catalytic activity in comparison with the parent framework. Alternatively, the catalytic activity can be influenced by the introduction of additional framework active sites [17]. Maksimchuk et al. reported the encapsulation of polyoxometalates into the nanocages of the MIL-101 framework [18]. The resulting material demonstrated a good catalytic activity for the epoxidation of various alkenes. Alkordi et al. encapsulated metalloporphyrins into zeolite-like MOFs which enhanced the catalytic activity for cyclohexane oxidation [19]. A third approach is to bring new catalytically active sites into the framework by a post-modification of the embedded functional groups [20]. Ingleson et al. reported the two steps modification of IRMOF-3 to an imine grafted $VO(acac)_2$ complex [21]. However, the resulting catalyst showed a rather low catalytic activity and stability for the oxidation of cyclohexene. The group of Battacharjee reported a more straightforward one step functionalization of the IRMOF-3 with $Mn(acac)_2$ [22]. Although a good catalytic and stability performance was obtained, the yield of the grafted complex was rather low (8%).

In our previous studies, we demonstrated that vanadium based MOFs (MIL-47 and COMOC-3), with saturated vanadium sites have a remarkable catalytic activity in the liquid phase epoxidation of cyclohexene with tert-Butyl hydroperoxide (TBHP) as oxidant [23–25]. However, both the experimental results and theoretical calculations showed that the catalytic cycle starts with the breaking of at least one V-carboxylate bond to coordinate the peroxide. The structural defects created during this process

* Corresponding author. Tel.: +32 9 264 43 56; fax: +32 9 264 49 96.
** Corresponding author. Tel.: +32 9 264 44 42; fax: +32 9 264 49 83.
E-mail addresses: Henk.Vrielinck@ugent.be (H. Vrielinck), Pascal.Vandervoort@ugent.be (P. Van Der Voort).

0920-5861/$ – see front matter © 2012 Elsevier B.V. All rights reserved.
http://dx.doi.org/10.1016/j.cattod.2012.09.037

contribute to the catalytic performance. Hence, a small amount of leaching was observed in the start of the catalysis. Our objective is to prevent leaching while maintaining or enhancing the catalytic performance. Therefore, we opted for a milder system using O_2 as oxidant in combination with cyclohexanecarboxaldehyde as a co-oxidant. To the best of our knowledge, a Ti grafted V-MOF has not been reported so far. Nevertheless, bimetallic Ti–V catalysts are reported to have a synergistic effect in oxidation catalysis [26].

In this contribution, we report a bimetallic V/Ti-MOF via post-functionalization of the V-MOF, NH_2-MIL-47 with a Titanylacetylacetonate complex (denoted as NH_2-MIL-47 [Ti] hereafter) (see Fig. 1). The obtained NH_2-MIL-47 [Ti] was examined in the oxidation of cyclohexene and was compared with the non-functionalized V-MOF as well as with the homogeneous $TiO(acac)_2$ catalyst. Additionally regeneration and stability tests were carried out. In our previous study of the catalytic activity of MIL-47 in the oxidation of cyclohexene with TBHP as oxidant, we used X-band (9.8 GHz) Electron Paramagnetic Resonance (EPR) measurements at room temperature (RT) to monitor the evolution in the fraction of V-ions in the paramagnetic +IV valence state [24]. We observed a reduction of the V^{+IV} concentration by about 20% in the first few hours of reaction, as a result of $V^{+IV} \rightarrow V^{+V}$ oxidation, confirming a radical parallel reaction pathway suggested by density functional theory (DFT) calculations. Similar EPR experiments are performed in this study in order to gain insight in the catalytic reaction mechanisms. In view of the absence of hyperfine (HF) structure in the spectra, the X-band measurements are complemented with *Q*-band experiments (34 GHz) and spectral simulations (Easyspin [27] library in Matlab®) in order to corroborate the assignment of the spectrum to V^{+IV}.

2. Materials and methods

2.1. General procedures

All chemicals were bought from Sigma–Aldrich and used without further purification. X-Ray Fluoresence (XRF) measurements were performed on a NEX CG from Rigaku using a Mo X-ray source. X-ray powder diffraction (XRPD) patterns were collected on a ARL X'TRA X-ray diffractometer with Cu-Kα radiation of 0.15418 nm wavelength and a solid state detector. The Cross Polarization Magic Angle Spinning Nuclear Magnetic Resonance (^{13}C CP/MAS NMR) spectra were recorded at 100.6 MHz on a Bruker AVANCE-400 WB spectrometer at RT. The samples were spun at 13 kHz. An overall 10,000 free induction decays were accumulated with 4 s of recycle time. Chemical shifts were measured relative to a tetramethylsilane standard. The ^1H NMR spectrum was recorded on a Bruker AVANCE DRX500 NMR spectrometer (500 MHz). Diffuse Reflectance Infrared Fourier Transform Spectroscopy (DRIFTS) measurements were recorded on a Thermo Nicolet 6700 FT-IR spectrometer equipped with a N_2 cooled MCT-A (mercury–cadmium–tellurium) detector. Nitrogen adsorption experiments were measured at −196 °C using a Belsorp mini II gas analyzer. The reaction products were identified with a TRACE GC × GC (Thermo, Interscience), coupled to a TEMPUS TOF-MS detector (Thermo, Interscience). The first column consists of a dimethyl polysiloxane package and has a length of 50 m, with an internal diameter of 0.25 mm, whereas the second column has a length of 2 m with an internal diameter of 0.15 mm. The package of the latter is a 50% phenyl polysilphenylene-siloxane. Helium was used as carrier gas with a constant flow (1.8 mL/min). An ultra-fast gas chromatograph (GC) equipped with a flame ionization detector (FID) and a 5% diphenyl/95% poly-dimethylsiloxane column with 10 m length and 0.10 mm internal diameter was used to follow the conversions of the products during the catalytic tests. Helium was used as carrier gas, and the flow rate was programmed as 0.8 mL/min.

2.2. Synthesis of NH_2-MIL-47 [Ti]

In a first step NH_2-MIL-47 was prepared *via* a microwave synthesis route. Typically 1.7 mmol VCl_3 was mixed with 1.7 mmol 2-aminoterephthalic acid in 3.02 mL·H_2O. The reaction was carried out at 150 °C for 20 min. Afterwards, an extraction in dimethylformamide (DMF) was performed at 125 °C for 90 min to remove unreacted linker.

In a second step $TiO(acac)_2$ was grafted onto the V-MOF. Different temperatures and reaction times have been applied as shown in Table S. 1 of the Supporting Information. In each experiment 0.0785 g $TiO(acac)_2$ was dissolved in 30 mL of dry toluene. After stirring the solution for 4 h at 55 °C, 0.15 g NH_2-MIL-47 was added to the solution. Subsequently this mixture was stirred at a certain temperature (55 °C, 70 °C and 90 °C) for 20 or 40 h under an inert argon atmosphere. Hereafter, the MOF was filtered on a combined nylon-membrane filter and washed several times with acetone to remove unreacted $TiO(acac)_2$. Afterwards the solid was dried overnight under vacuum.

2.3. Catalytic setup

In a typical catalytic test, a schlenk flask was loaded with 40.0 mL of acetonitrile as solvent, 7.0 mL cyclohexene (substrate) and 8.4 mL 1,2,4-trichlorobenzene used as internal standard. Oxygen (99.9% pure) was applied as the oxidant in combination with the co-oxidant cyclohexanecarboxaldehyde (7.6 mL). A constant oxygen flow of 7 mL/min was bubbled through the solution by means of a mass flow controller. Blanc reactions were carried out in the absence of catalyst which showed no conversion of cyclohexene. All the catalytic tests were carried out at a temperature of 40 °C in a schlenk flask equipped with a liquid condenser coupled with recirculating cooling liquid at −4 °C to prevent evaporation of the reaction mixture. Aliquots were gradually taken out of the mixture, diluted with 500 μl ethylacetate, and subsequently analyzed by GC–FID.

2.4. EPR measurements

For quantitative EPR analysis, spectra of dry powders, contained in quartz tubes with an outer diameter of 4 mm, filled to a height of approximately 6 mm (30–35 mg), were recorded at RT using a Bruker ESP300E X-band spectrometer (ER 4102-ST rectangular cavity). In the bottom part of the EPR cavity an open quartz tube was fixed, on which the sample tubes rested, in order to ensure reproducible positioning. The microwave frequency was measured using a HP 5350 B microwave frequency counter. The magnetic field was modulated at 100 kHz with a peak-to-peak amplitude of 0.1 mT and the microwave power was set to 2 mW, avoiding saturation. A broad magnetic field range was swept (350 mT) around the free electron *g*-value (2.0023). All spectra were normalized to a microwave frequency of 9.77 GHz for comparison and corrected for the background spectrum of the empty cavity. For comparison of intensities, the spectra were divided by the sample mass. In order to resolve the anisotropy, selected powders were also measured in Q-band (≈34 GHz) at RT on a Bruker Elexsys E500 spectrometer equipped with a Pendulum CNT-90XL frequency counter (spectra normalized to 33.98 GHz). These measurements were performed on powders contained in 2 mm outer diameter quartz tubes filled to a height of about 2 mm.

Please cite this article in press as: K. Leus, et al., Ti-functionalized NH_2-MIL-47: An effective and stable epoxidation catalyst, Catal. Today (2012), http://dx.doi.org/10.1016/j.cattod.2012.09.037

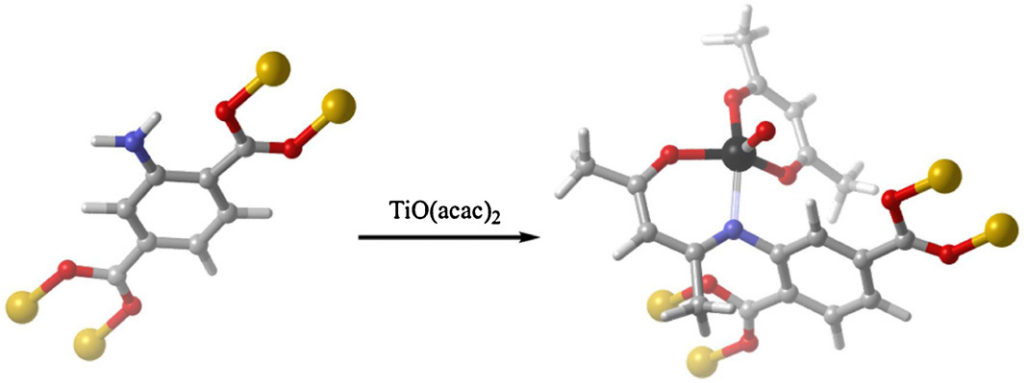

Fig. 1. Schematic representation of the post-functionalization of NH_2-MIL-47 with a Titanylacetylacetonatecomplex (the carbon atoms are shown in gray, the oxygen atoms are depicted in red and the N, Ti and V atoms are shown in blue, black and yellow, respectively). (For interpretation of the references to color in the artwork, the reader is referred to the web version of the article.)

2.5. Computational details

Ab initio calculations are performed with the gaussian09 program [28]. All models were optimized with a B3LYP [29,30] functional using a 6–31 + G(d) Pople basis set. Vibrational frequency calculations were done at the same level of theory. To compare the calculated frequencies with the experimental DRIFTS spectrum a scale factor of 0.9648 was imposed, as proposed by Merrick et al. [31].

3. Experimental results and discussion

3.1. Characterization of the functionalized materials

3.1.1. XRPD analysis and determination of the Ti loading

By means of XRF the Ti loading was determined of the functionalized MOF materials (see Table S. 1). Approximately the same loading was obtained in each experiment, with an average of 1.25 mmol Ti/g, which indicates that almost 30% of the $-NH_2$ groups on the organic linker are modified. It should be noted that this loading is much higher compared to the earlier reported one step functionalization of $Mn(acac)_2$ on IRMOF-3, which was approximately 0.23 mmol Mn/g [22]. Furthermore, the crystallinity of all the obtained Ti-grafted materials was verified by XRPD measurements (see Fig. S.1 Supporting Information). As can be seen from this figure, the XRPD pattern of each functionalized material presents the pure phase of the non-functionalized NH_2-MIL-47. This explicitly shows that the framework integrity of the parent MOF was well preserved during the post-functionalization.

3.1.2. DRIFTS, ^{13}C CP/MAS NMR and ^{1}H NMR measurements

DRIFTS, ^{13}C CP/MAS and ^{1}H NMR measurements were carried out to verify if the $TiO(acac)_2$ complex was actually grafted onto the V-MOF. We selected the sample NH_2-MIL-47 [Ti], 70 °C, 20 h, for a detailed characterization and subsequent catalytic studies. In Fig. 2 the ^{13}C CP/MAS NMR spectra of NH_2-MIL-47 and

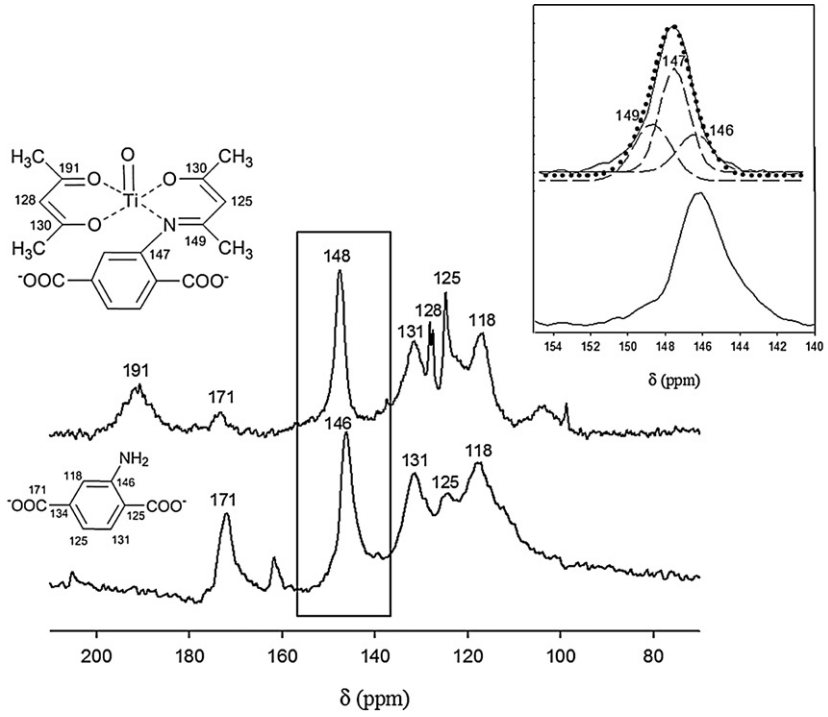

Fig. 2. ^{13}C CP/MAS NMR spectra of NH_2-MIL-47 and NH_2-MIL-47 [Ti]. (INSET): detailed NMR spectrum of the signal at 148 ppm and its deconvolution.

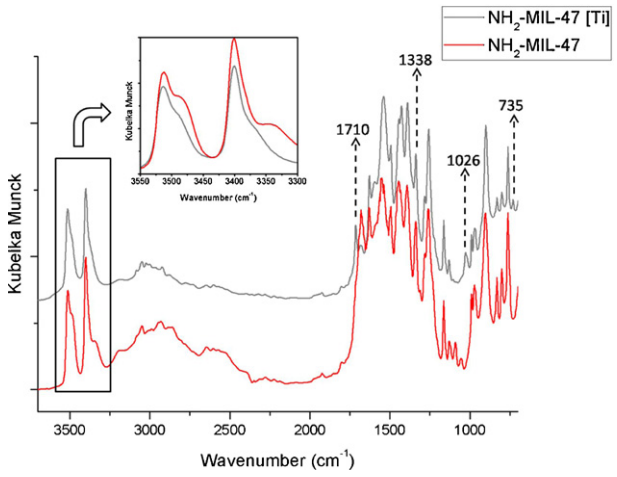

Fig. 3. DRIFTS spectra of NH_2-MIL-47 (shown in red) and NH_2-MIL-47 [Ti], 70 °C, 20 h(shown in black) INSET: detailed DRIFTS spectra of both materials in the region 3550–3300 cm^{-1}. The spectra were normalized to the vibration at 800 cm^{-1} which corresponds to the aromatic C—H out of plane bend mode. (For interpretation of the references to color in the artwork, the reader is referred to the web version of the article.)

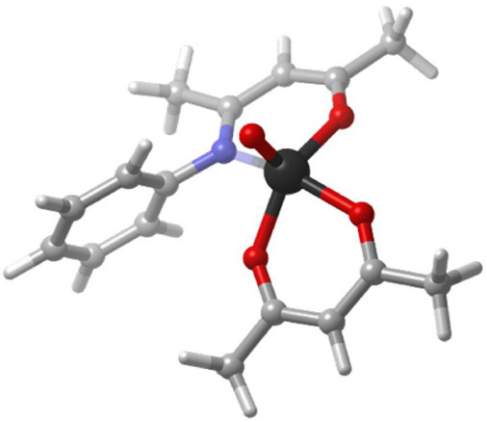

Fig. 4. Model used in the calculation of the IR vibrations after post-functionalization with the $TiO(acac)_2$ moiety (the C atoms are shown in gray, N atoms in blue, and the O and Ti atoms are depicted in red and black, respectively). (For interpretation of the references to color in the artwork, the reader is referred to the web version of the article.)

NH_2-MIL-47 [Ti] are presented. The ^{13}C CP/MAS NMR spectrum of NH_2-MIL-47 gave several signals at 118, 125, 131 and 146 ppm associated with different sp^2 carbons of the organic linker and one peak at 171 ppm assigned to the carbonyl groups of the amino terephthalate linker [32]. In the non-functionalized NH_2-MIL-47 an additional signal at 162 ppm confirmed the incomplete removal of solvent (DMF) used in the synthesis of the material. After functionalization, NH_2-MIL-47[Ti] showed new bands which corroborate the presence of the grafted $TiO(acac)_2$ complex on NH_2-MIL-47. An intense signal appeared at ca. 148 ppm. As can be seen from Fig. 2 (inset), this signal could be deconvoluted into 3 peaks: the signal at 146 ppm corresponds to the C—N bond (non-functionalized material), whereas the signal at 147 and 149 ppm can be associated to the C—N and C═N groups of the bimetallic MOF, respectively [32]. This proves the success of the post-functionalization. Moreover, the NH_2-MIL-47 [Ti] showed several peaks in the aromatic region (120–130 ppm) and a new peak at ca. 191 ppm, which correspond to the C═C and C═O groups of the titanylacetylacetonate complex, respectively [32]. The ^1H NMR spectrum (see Fig. S4) of the digested NH_2-MIL-47 [Ti] shows peaks at 2.06, 1.94 and 1.85 ppm due to the —CH_3 groups further confirming the presence of acac and imine-functionalized acac ligands grafted onto NH_2-MIL-47.

The DRIFTS spectra of the NH_2-MIL-47 and NH_2-MIL-47[Ti], 70 °C, 20 h are shown in Fig. 3 (the DRIFTS spectra of the other materials are presented in Fig. S.2). It is clear that the characteristic vibrations of the parent MOF are still present. However, after the post-functionalization a decrease in intensity of some vibrations is observed, pointing toward a decrease in concentration of the -NH_2 groups. The typical vibrations of the benzene linker at 1510–1450 cm^{-1} (aromatic ring stretch), 1225–950 cm^{-1} (aromatic C—H in plane bend) and 900–670 cm^{-1} (aromatic C—H out of plane bend) [33] remain unchanged. Furthermore, the symmetric and asymmetric —CO_2 stretching vibrations in the region 1463–1415 $cm^{-1}$and 1616–1597 cm^{-1} are still present after grafting [34].

The principal changes in the spectrum before and after post-functionalization can be connected to the amine moiety. To obtain more insight in these changes, molecular modeling calculations were applied. The model of the catalyst was built by isolating the aromatic part of the linker with a $TiO(acac)_2$ substituent, as shown in Fig. 4. For comparison, the NH_2-MIL-47 was modeled as aniline. Only the relevant parts of the structure have been taken into account to calculate the spectra. Therefore, in both models the carboxylic acid group and its coordination with vanadium was not included since it would not contribute any relevant information to the calculated spectrum. The absorbance due to the vibrations at 1338 cm^{-1}(C—N stretch) and the doublet at 3494 cm^{-1} and 3386 cm^{-1}(NH_2 asymmetric and symmetric stretch) decrease in comparison to the non-functionalized V-MOF [35,36]. Also the skeletal vibration bands that contain NH_2 rocking at 1050 cm^{-1} and 1100 cm^{-1} become less intense due to a partial modification of the amine groups. The presence of the $TiO(acac)_2$ modification can be seen by the vibrations at 735 cm^{-1}(C—C—H twisting) and 1026 cm^{-1}(C—CO—C wagging). The C═N vibration cannot be seen since it overlaps with the vibrations from the parent MOF between 1600 cm^{-1} and 1700 cm^{-1}. The new peak that appears at 1710 cm^{-1} could not be assigned with this model. This vibration could be due to free C═O vibrations, which are the consequence of some $TiO(acac)_2$ complexes that break during the post-functionalization. This would result in a ketone substituent which is not coordinated with titanium on the MOF.

3.1.3. Nitrogen sorption measurement

In Fig. 5 the nitrogen adsorption isotherms of NH_2-MIL-47 and NH_2-MIL-47 [Ti], 70 °C, 20 h are compared. The Langmuir surface area of the non-functionalized and post-functionalized material is 650 m^2/g and 190 m^2/g respectively. Despite the high loading of Ti (approximately 30%), the post-functionalized MOF retains a partial

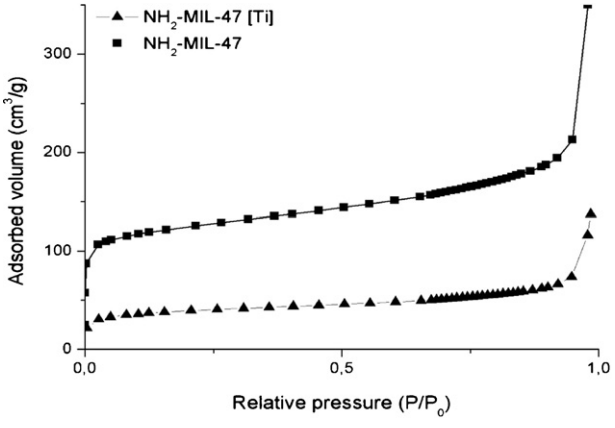

Fig. 5. Nitrogen adsorption isotherms of NH_2-MIL-47 and NH_2-MIL-47 [Ti].

Please cite this article in press as: K. Leus, et al., Ti-functionalized NH_2-MIL-47: An effective and stable epoxidation catalyst, Catal. Today (2012), http://dx.doi.org/10.1016/j.cattod.2012.09.037

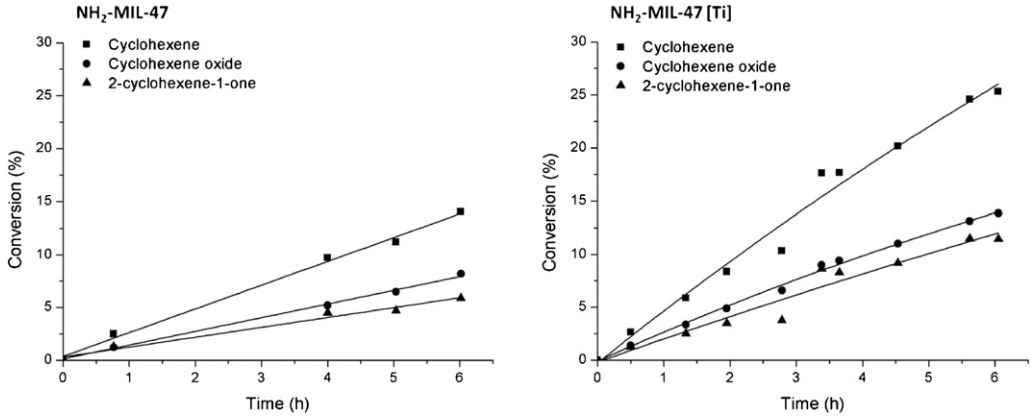

Fig. 6. Cyclohexene conversion (■) and the yield of cyclohexene oxide (●) and 2-cyclohexene-1-one (▲) for NH_2-MIL-47 and NH_2-MIL-47 [Ti] using acetonitrile as solvent and oxygen as oxidant in combination with the co-oxidant cyclohexanecarboxaldehyde at a temperature of 40 °C. In both experiments a V loading of 0.42 mmol was applied.

porosity. In addition, the calculated pore volume of the parent and post-modified MOF is 0.30 mL/g and 0.10 mL/g, respectively.

3.2. Evaluation of the catalytic performance in the oxidation of cyclohexene

The catalytic performance of NH_2-MIL-47 and NH_2-MIL-47 [Ti], 70 °C, 20 h was evaluated in the oxidation of cyclohexene. To make a fair comparison of both materials, the catalyst loading was chosen such that the number of V-sites was equal in the two experiments. Fig. 6 depicts the cyclohexene conversion and the detailed product distribution of both catalysts in the first run. Several features can be deduced from this figure. (1) A cyclohexene conversion of approximately 14.1% and 25% is observed respectively for the non-functionalized and bimetallic material after 6 h of reaction. This clearly shows that the bimetallic MOF exhibits a significantly higher catalytic performance than the (monometallic) V-MOF due to the presence of the extra active sites. (2) Moreover, faster conversion is observed for the bimetallic MOF. After 2 h of reaction, 10% of cyclohexene is already converted, whereas NH_2-MIL-47 shows only 6% of conversion. (3) Finally, it can be noted that both materials show only 2 products: cyclohexene oxide and the radical product 2-cyclohexene-1-one, which are produced in almost equal amounts. In Section 3.5 reaction mechanisms are proposed that explain this product distribution.

Additionally, the homogenous catalyst $TiO(acac)_2$ has been tested using the same experimental conditions as for the MOF materials. The same amount of Ti has been used as in the post-functionalized material. The conversion pattern of this homogeneous catalyst is depicted in Fig. 7. After 6 h of reaction a cyclohexene conversion of 25% is reached, which is practically the same as for the Ti/V-MOF. It is interesting to note that the product distribution observed for the homogeneous catalyst is very similar as for the NH_2-MIL-47 and NH_2-MIL-47 [Ti]: almost equal percentages of the cyclohexene oxide and the ketone are observed.

3.3. Stability and regenerability of the catalysts

To test the regenerability of the V-MOFs, two additional runs have been executed on both materials. In Fig. 8, the cyclohexene conversion is shown after each run for the two catalysts, whereas in Table 1 the TON, TOF and leaching percentage are presented after each run for both materials. As can be seen from Fig. 8, the cyclohexene conversion for the post-functionalized material is slightly enhanced after the first run which is due to the generation of the extra catalytic V^{+V} sites (see Section 3.4). However, for the non-functionalized V-MOF a significantly higher cyclohexene conversion is observed for the 2nd and the 3rd run (30% and 24%). This is due to the V leaching in each run as can be noted from Table 1. In each run a small amount of V-leaching is observed (1,8%, 2.5% and 3.5%) which gives rise to additional defects in the framework structure. Extra defects present in the structure can significantly influence the catalytic performance in the additional

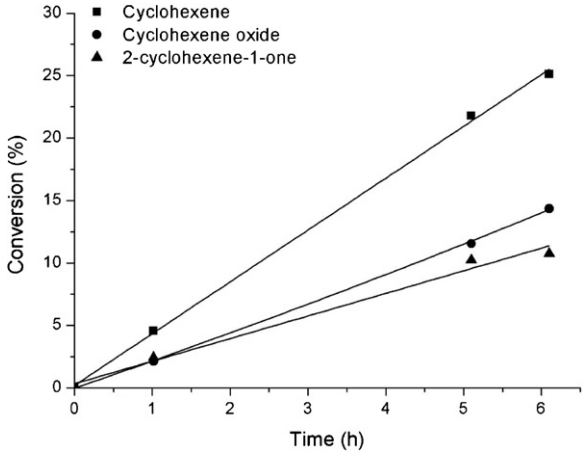

Fig. 7. Cyclohexene conversion (■) and the yield of cyclohexene oxide (●) and 2-cyclohexene-1-one(▲) for $TiO(acac)_2$ using acetonitrile as solvent and oxygen as oxidant in combination with the co-oxidant cyclohexanecarboxaldehyde at a temperature of 40 °C. The same Ti loading was applied as for the NH_2-MIL-47 [Ti] (0.22 mmol Ti).

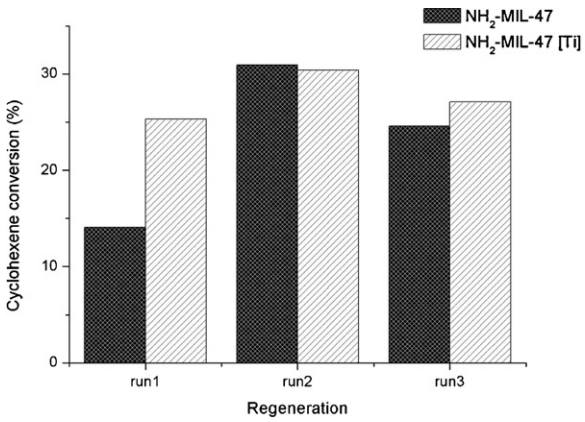

Fig. 8. Cyclohexene conversion for the executed additional runs on NH_2-MIL-47 and NH_2-MIL-47 [Ti].

Please cite this article in press as: K. Leus, et al., Ti-functionalized NH_2-MIL-47: An effective and stable epoxidation catalyst, Catal. Today (2012), http://dx.doi.org/10.1016/j.cattod.2012.09.037

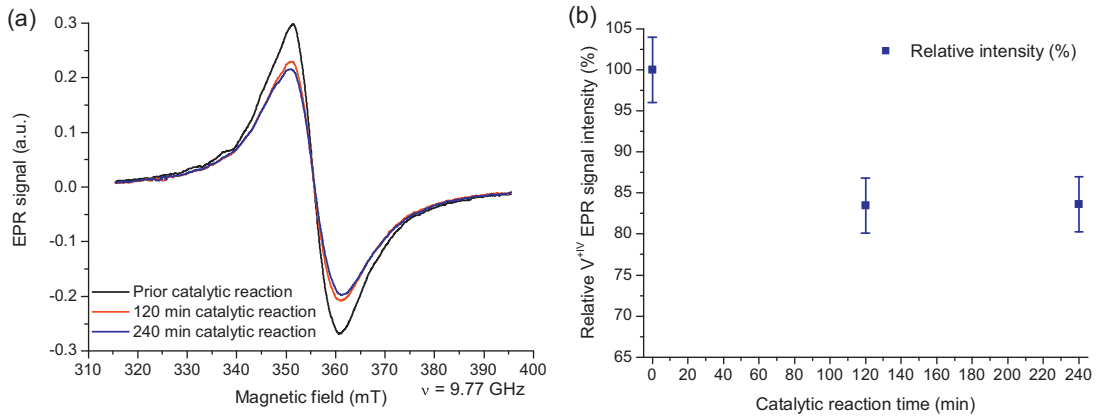

Fig. 9. (a) X-band EPR spectra at RT of the NH_2-MIL-47 [Ti] samples before and after catalysis; (b) Relative V^{+IV} EPR signal intensity with respect to the signal of NH_2-MIL-47 [Ti] prior to catalysis. The error (1σ) is estimated at 4% (see text). (For interpretation of the references to color in the artwork, the reader is referred to the web version of the article.)

runs [24]. The NH_2-MIL-47 [Ti] did not show any detectable Ti or V leaching, which clearly demonstrates that the original MOF after post-functionalization becomes more stable. The exact reason for the enhanced leaching stability is currently unclear. Both shielding effects and electronic effects may influence the leaching behavior and would require advanced modeling techniques [37]. This falls beyond the scope of this current paper.

Comparison of the XRPD pattern of NH_2-MIL-47 [Ti] before catalysis and after each run (see Fig. S.3) clearly shows that the framework integrity of the MOF is well preserved.

3.4. EPR measurements

The aim of the EPR measurements is gaining insight in the reaction mechanisms by monitoring the fraction of paramagnetic V^{+IV} ions in the catalyst. Fig. 9 a shows the RT X-band spectra of NH_2-MIL-47 [Ti] dry powder samples before and after 2 and 4 h of catalysis. The spectra of the samples prior to and after catalysis appear as single broad lines exhibiting widths of about 9.2 mT before and 10.4 mT after catalysis. No ^{51}V hyperfine (HF) structure is resolved in the spectra. The line position in the X-band spectra is practically the same for all samples and already suggests a signal assignation to V^{+IV} ($g = 1.96 < g_e = 2.0023$) [38]. Furthermore, spectra were recorded at higher microwave frequency (Q-band), which partially resolves the anisotropy of the $(V^{+IV}=O)\,O_4$ complexes. In Fig. 10 the RT Q-band EPR spectrum of NH_2-MIL-47 [Ti] is compared with that of NH_2-MIL-47 and MIL-47. Spectrum simulations show that in all three samples the paramagnetic species have (approximately) axial symmetry. The $g_{||}$ (along the V=O bond direction) and $g_{\perp}$ values obtained through fitting of the spectra are listed in Table 2. These values are typical for V^{+IV} species [38] and are in very good agreement with earlier EPR reports on V-MOFs [39]. It is worth noting that both in the work of Meilikhov et al. [39] and in our own previous investigations of V-MOFs [24,25], no HF structure

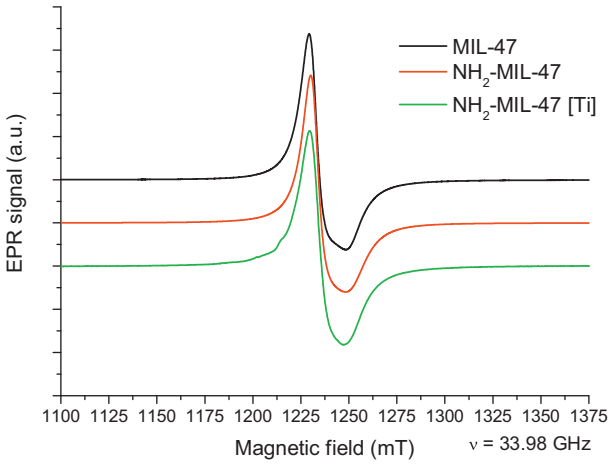

Fig. 10. Q-band (33.98 GHz) EPR spectrum of NH_2-MIL-47 [Ti] compared with the spectra of non-functionalized NH_2-MIL-47 and of MIL-47 at RT. (For interpretation of the references to color in the artwork, the reader is referred to the web version of the article.)

was resolved in the spectra, most probably as a result of interactions between spins in these paramagnetically concentrated samples. The number of paramagnetic centers in the samples was estimated by comparing the signal intensity with that of a $VO(acac)_2$ grafted silica sample with known V^{+IV} loading. It was found to be comparable to the number of V-sites in the catalyst, indicating that at RT EPR provides information on the majority of the metal V-sites, and not only on a minority fraction, e.g. corresponding to defects.

The intensity of the RT X-band spectra was evaluated by double integration of the EPR spectra over a range of 80.0 mT centered on the broad EPR line, in order to avoid errors due to non-perfect background correction in the broader range recorded. The data points in Fig. 9b represent the relative intensity with respect to the signal of NH_2-MIL-47 [Ti] prior to catalytic reaction. The error (one standard deviation) is estimated at 4%, combining the effects of variations in consecutive measurements (sample positioning) and day-by-day changes in the spectrometer sensitivity. One observes that within

Table 1
TON, TOF and leaching percentage after each run for both V-based catalysts.

Sample	TON[a]	TOF[b] (h^{-1})	Leaching (%)
NH_2-MIL-47			
Run 1	17.7	6.0	1.8
Run 2	44.6	14.1	2.5
Run 3	63.9	10.4	3.5
NH_2-MIL-47 [Ti]			
Run 1	39.5	7.5	0
Run 2	44.8	12.1	0
Run 3	49.5	1.1	0

[a] TON was calculated after 6 h of reaction.
[b] TOF was calculated after 30 min of reaction.

Table 2
Best fit principal g values for the V^{+IV} centers in MIL-47, NH_2-MIL-47 and NH_2-MIL-47 [Ti] at RT (see Fig. 10).

T	Sample	$g_{\perp}$	$g_{||}$
RT	MIL-47	1.972	1.941
	NH_2-MIL-47	1.970	1.940
	NH_2-MIL-47 [Ti]	1.970	1.940

Please cite this article in press as: K. Leus, et al., Ti-functionalized NH_2-MIL-47: An effective and stable epoxidation catalyst, Catal. Today (2012), http://dx.doi.org/10.1016/j.cattod.2012.09.037

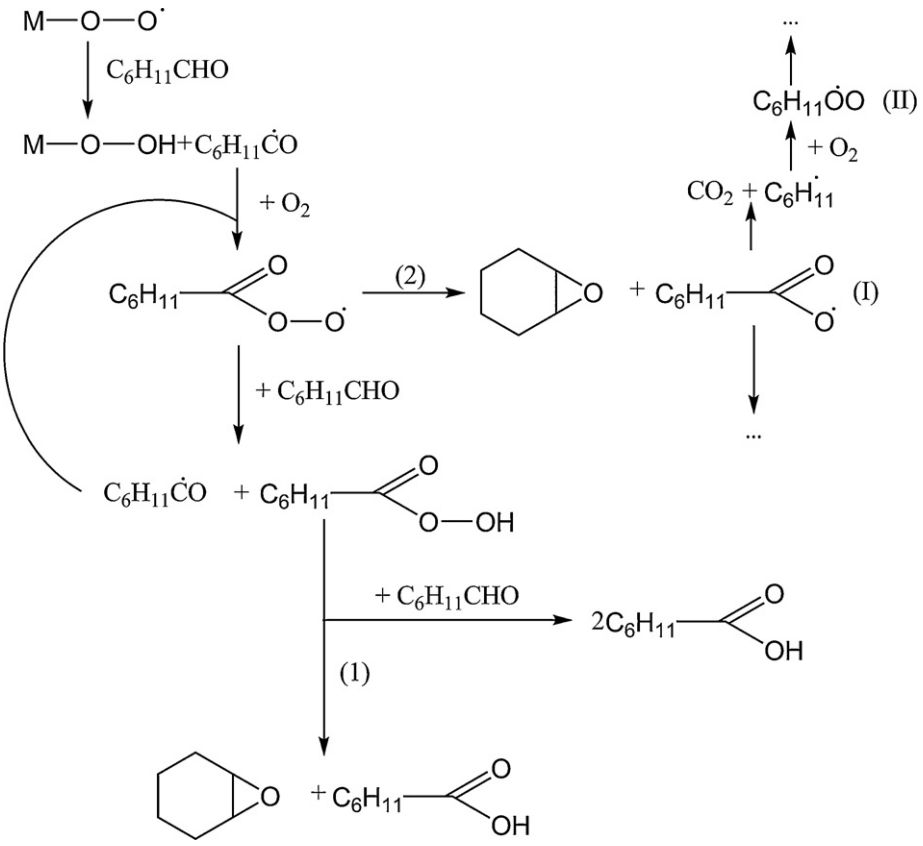

Scheme 1. General mechanism of the epoxidation with O_2 and aldehydes, most termination steps where omitted for clarity.

the first 2 h of catalysis, the spectrum intensity decreases about 17%. Thereafter it remains stable or decreases more slowly. A very similar behavior was observed for MIL-47 in the oxidation of cyclohexene with TBHP/decane as oxidant [24]. Hence, we propose a similar interpretation: in the first few hours of catalysis a fraction of the V^{+IV} centers is oxidized to diamagnetic V^{+V} centers. Mechanistic considerations in Section 3.5 suggest a radical parallel pathway, involving a partial oxidation of the V-metal sites.

3.5. Reaction mechanisms

Based on the above described EPR and catalytic results a plausible reaction mechanism is proposed. The mechanism of oxidation using molecular oxygen and a sacrificial co-oxidant has been the subject of many studies. A radical mechanism involving a peracid radical as primary oxidizing species has been generally accepted (Scheme 1) [40]. The role of the catalyst is considered to be the activation of molecular oxygen by the generation of radicals. However, a metal-oxygen moiety can be present as alternative, direct oxidizing species in the metal-catalyzed system. This oxidation pathway is generally accepted for late transition metals [41,42]. Nevertheless, for metals like titanium and vanadium, this pathway is less likely as described in Sheldon et al. [43]. The presence of metal-oxo species could explain the decrease of the V^{+IV} signal intensity in the EPR measurements since the generation of vanadium-oxo species is accompanied by an oxidation to V^{+V}, which corresponds to what was already reported for the V-MIL-47 in the cyclohexene oxidation using TBHP as oxidant [24].

Another argument in favor for the mechanism shown in Scheme 1 is the presence of cyclohexanone in the product mixture. This is due to the formation of the peroxide radical ((II) in Scheme 1), followed by the formation of peroxide by a hydrogen abstraction. Afterwards, the obtained peroxide can react with another peroxide to form the cyclohexanone and oxygen (see Scheme 2).

This type of reaction generally exhibits a high (>80%) selectivity toward the epoxide when it is catalyzed by complexes where the metal can only have a low oxidation state (maximum II or III) [44]. A MOF containing the same metals as those mostly used as homogeneous catalysts (Ni, Cu, Co) for this reaction gave similar results [41]. In the present system however, the selectivity toward the epoxide is significantly lower. It is known that the presence of carboxylic acid radicals and peroxo radicals ((I) and (II) in Scheme 1) can lead to oxidation in the allylic position [40,41]. It is likely that these intermediates are stabilized by titanium and vanadium in the catalyst, leading to a decreased selectivity. Furthermore, the presence of M=O species and peroxide moieties can lead to the formation

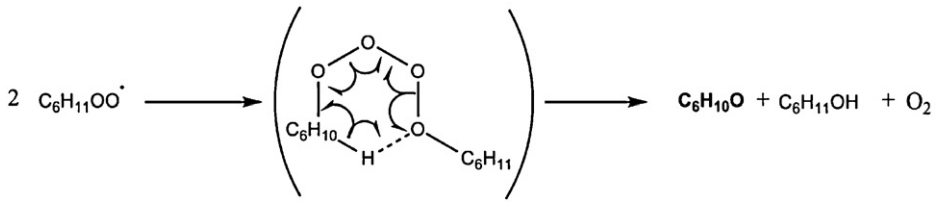

Scheme 2. formation of cyclohexanone, which was observed in the product mixture.

Please cite this article in press as: K. Leus, et al., Ti-functionalized NH_2-MIL-47: An effective and stable epoxidation catalyst, Catal. Today (2012), http://dx.doi.org/10.1016/j.cattod.2012.09.037

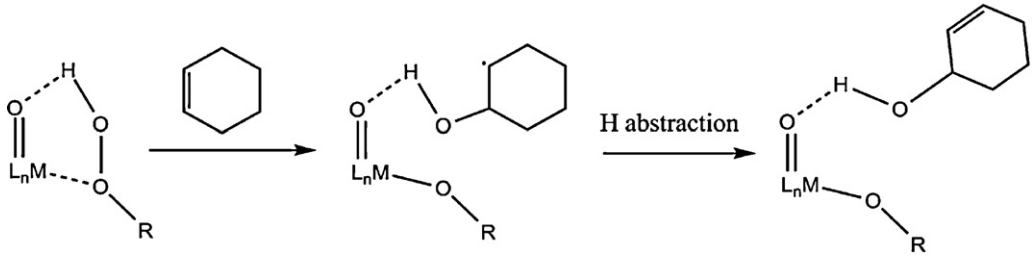

Scheme 3. Pathway to cyclohexenol formation.

of cyclohexenol as shown in Scheme 3. Cyclohexenol can then be oxidized further to 2-cyclohexene-1-one, this conversion was also shown by Murahashi et al. [44].

4. Conclusions

We succeeded in the post-functionalization of NH_2-MIL-47 with $TiO(acac)_2$. ^{13}C CP/MAS NMR, ^1H NMR and DRIFTS measurements clearly established the effectiveness of the grafting procedure, whereas XRPD measurements proved the stability of the bimetallic MOF during the grafting process. The obtained NH_2-MIL-47 [Ti] exhibits a significantly higher cyclohexene conversion compared to the non-functionalized material, probably mainly due to the extra active sites. Furthermore, no leaching of V or Ti was detected. Regenerability tests have shown that only a slight increase in cyclohexene conversion is observed during the first 3 runs. EPR measurements indicate that about 17% of the V^{+IV} sites are oxidized to V^{+V} in the first two hours of catalysis. In agreement with the latter, the general mechanism of the epoxidation with O_2 and aldehydes shows the generation of vanadium-oxo species which is accompanied by a partial oxidation of the V centers toward V^{+V}.

Acknowledgments

K.L. is grateful to the Long Term Structural Methusalem Grant No. 01M00409 funding by the Flemish Government. Furthermore, this research is co-funded by Ghent University, GOA Grant No. 01G00710, the Research Foundation Flanders (FWO-Vlaanderen) through Grant No. G.0700.08, BELSPO in the frame of IAP 6/27 and the European Research Council (FP7(2007–2013) ERC Grant No. 240483). Computational resources (Stevin Supercomputer Infrastructure) and services were provided by Ghent University. The authors would like to thank the research group FQM-346 and the SCAI from the University of Córdoba (Spain) for the ^{13}C CP/MAS NMR measurements. The NMRSTR research group of Ghent University is acknowledged for performing the ^1H NMR measurements.

Appendix A. Supplementary data

Supplementary data associated with this article can be found, in the online version, at http://dx.doi.org/10.1016/j.cattod.2012.09.037.

References

[1] J.R. Li, J. Sculley, H.C. Zhou, Chemical Reviews 112 (2012) 869–932.
[2] J. Sculley, D.Q. Yuan, H.C. Zhou, Energy and Environmental Science 4 (2011) 2721–2735.
[3] J.R. Li, Y.G. Ma, M.C. McCarthy, J. Sculley, J.M. Yu, H.K. Jeong, P.B. Balbuena, H.C. Zhou, Coordination Chemistry Reviews 255 (2011) 1791–1823.
[4] D. Farrusseng, S. Aguado, C. Pinel, Angewandte Chemie International Edition 48 (2009) 7502–7513.
[5] J. Lee, O.K. Farha, J. Roberts, K.A. Scheidt, S.T. Nguyen, J.T. Hupp, Chemical Society Reviews 38 (2009) 1450–1459.
[6] Y. Liu, W.M. Xuan, Y. Cui, Advanced Materials 22 (2010) 4112–4135.
[7] A. Corma, H. Garcia, F.X.L. Xamena, Chemical Reviews 110 (2010) 4606–4655.
[8] M.G. Goesten, J. Juan-Alcaniz, E.V. Ramos-Fernandez, K.B.S.S. Gupta, E. Stavitski, H. van Bekkum, J. Gascon, F. Kapteijn, Journal of Catalysis 281 (2011) 177–187.
[9] W.Q. Kan, B. Liu, J. Yang, Y.Y. Liu, J.F. Ma, Crystal Growth and Design 12 (2012) 2288–2298.
[10] J. Rocha, L.D. Carlos, F.A.A. Paz, D. Ananias, Chemical Society Reviews 40 (2011) 926–940.
[11] H. Liu, Y.G. Zhao, Z.J. Zhang, N. Nijem, Y.J. Chabal, H.P. Zeng, J. Li, Advanced Functional Materials 21 (2011) 4754–4762.
12 Y.G. Zhao, H.H. Wu, T.J. Emge, Q.H. Gong, N. Nijem, Y.J. Chabal, L.Z. Kong, D.C. Langreth, H. Liu, H.P. Zeng, J. Li, Chemistry – A European Journal 17 (2011) 5101–5109.
[13] T.K. Prasad, D.H. Hong, M.P. Suh, Chemistry – A European Journal 16 (2010) 14043–14050.
[14] J.P.S. Mowat, S.R. Miler, J.M. Griffin, V.R. Seymour, S.E. Ashbrook, S.P. Thompson, D. Fairen-Jimenez, A.M. Banu, T. Duren, P.A. Wright, Inorganic Chemistry 50 (2011) 10844–10858.
[15] C. Zlotea, D. Phanon, M. Mazaj, D. Heurtaux, V. Guillerm, C. Serre, P. Horcajada, T. Devic, E. Magnier, F. Cuevas, G. Ferey, P.L. Llewellyn, M. Latroche, Dalton Transactions 40 (2011) 4879–4881.
[16] F. Vermoortele, M. Vandichel, B. Van de Voorde, R. Ameloot, M. Waroquier, V. Van Speybroeck, D. De Vos, Angewandte Chemie International Edition 51 (2012) 4887–4890.
[17] S.M. Cohen, Chemical Reviews 112 (2012) 970–1000.
[18] N.V. Maksimchuk, K.A. Kovalenko, S.S. Arzumanov, Y.A. Chesalov, M.S. Melgunov, A.G. Stepanov, V.P. Fedin, O.A. Kholdeeva, Inorganic Chemistry 49 (2010) 2920–2930.
[19] M.H. Alkordi, Y.L. Liu, R.W. Larsen, J.F. Eubank, M. Eddaoudi, Journal of the American Chemical Society 130 (2008) 12639–12641.
[20] O.V. Zalomaeva, K.A. Kovalenko, Y.A. Chesalov, M.S. Mel'gunov, V.I. Zaikovskii, V.V. Kaichev, A.B. Sorokin, O.A. Kholdeeva, V.P. Fedin, Dalton Transactions 40 (2011) 1441–1444.
[21] M.J. Ingleson, J.P. Barrio, J.B. Guilbaud, Y.Z. Khimyak, M.J. Rosseinsky, Chemical Communications (23) (2008) 2680–2682.
[22] S. Bhattacharjee, D.A. Yang, W.S. Ahn, Chemical Communications 47 (2011) 3637–3639.
[23] K. Leus, I. Muylaert, M. Vandichel, G.B. Marin, M. Waroquier, P. Van der Voort, Chemical Communications 46 (2010) 5085–5087.
[24] K. Leus, M. Vandichel, Y.Y. Liu, I. Muylaert, J. Musschoot, S. Pyl, H. Vrielinck, F. Callens, G.B. Marin, C. Detavernier, P.V. Wiper, Y.Z. Khimyak, M. Waroquier, V. Van Speybroeck, P. Van der Voort, Journal of Catalysis 285 (2012) 196–207.
[25] Y.Y. Liu, K. Leus, M. Grzywa, D. Weinberger, K. Strubbe, H. Vrielinck, R. Van Deun, D. Volkmer, V. Van Speybroeck, P. Van der Voort, European Journal of Inorganic Chemistry 16 (2012) 2819–2827.
[26] I. Muylaert, J. Musschoot, K. Leus, J. Dendooven, C. Detavernier, P. Van der Voort, European Journal of Inorganic Chemistry (2) (2012) 251–260.
[27] S. Stoll, A. Schweiger, Journal of Magnetic Resonance 178 (2006) 42–55.
[28] M.J.T. Frisch, G.W. Schlegel, H.B. Scuseria, G.E. Robb, M.A. Cheeseman, J.R. Scalmani, G. Barone, V. Mennucci, B. Petersson, G.A. Nakatsuji, H. Caricato, M. Li, X. Hratchian, H.P. Izmaylov, A.F. Bloino, J. Zheng, G. Sonnenberg, J.L. Hada, M. Ehara, M. Toyota, K. Fukuda, R. Hasegawa, J. Ishida, M. Nakajima, T. Honda, Y. Kitao, O. Nakai, H. Vreven, T. Montgomery Jr., J.A. Peralta, J.E. Ogliaro, F. Bearpark, M. Heyd, J.J. Brothers, E. Kudin, K.N. Staroverov, V.N. Kobayashi, R. Normand, J. Raghavachari, K. Rendell, A. Burant, J.C. Iyengar, S.S. Tomasi, J. Cossi, M. Rega, N. Millam, N.J. Klene, M. Knox, J.E. Cross, J.B. Bakken, V. Adamo, C. Jaramillo, J. Gomperts, R. Stratmann, R.E. Yazyev, O. Austin, A.J. Cammi, R. Pomelli, C. Ochterski, J.W. Martin, R.L. Morokuma, K. Zakrzewski, V.G. Voth, G.A. Salvador, P. Dannenberg, J.J. Dapprich, S. Daniels, A.D. Farkas, O. Foresman, J.B. Ortiz, J.V. Cioslowski, J. Fox, D.J. Gaussian 09, {R}evision {A}. 02, Gaussian, Inc., Wallingford CT, 2009.
[29] A.D. Becke, Journal of Chemical Physics 98 (1993) 5648–5652.
[30] C.T. Lee, W.T. Yang, R.G. Parr, Physical Review B 37 (1988) 785–789.
31 J.P. Merrick, D. Moran, L. Radom, Journal of Physical Chemistry A 111 (2007) 11683–11700.
32 E. Pretsch, P. Bühlmann, C. Affolter, A. Herrera, R. Martínez, Determinaci on estructural de compuestos org anicos, Elsevier Masson (2001).
[33] J. Coates (Ed.), Interpretation of Infrared Spectra, A Practical Approach, 2000.
[34] T. Loiseau, C. Serre, C. Huguenard, G. Fink, F. Taulelle, M. Henry, T. Bataille, G. Ferey, Chemistry – A European Journal 10 (2004) 1373–1382.
[35] J. Gascon, U. Aktay, M.D. Hernandez-Alonso, G.P.M. van Klink, F. Kapteijn, Journal of Catalysis 261 (2009) 75–87.

[36] M. Kandiah, M.H. Nilsen, S. Usseglio, S. Jakobsen, U. Olsbye, M. Tilset, C. Larabi, E.A. Quadrelli, F. Bonino, K.P. Lillerud, Chemistry of Materials 22 (2010) 6632–6640.
[37] J.M. Ho, C.J. Easton, M.L. Coote, Journal of the American Chemical Society 132 (2010) 5515–5521.
[38] R. Pilbrow (Ed.), Transition Ion Electron Paramagnetic Resonance, Clarendon Press, Oxford, 1990.
[39] M. Meilikhov, K. Yusenko, A. Torrisi, B. Jee, C. Mellot-Draznieks, A. Poppl, R.A. Fischer, Angewandte Chemie International Edition 49 (2010) 6212–6215.
[40] B.B. Wentzel, P.L. Alsters, M.C. Feiters, R.J.M. Nolte, Journal of Organic Chemistry 69 (2004) 3453–3464.
[41] E. Angelescu, O.D. Pavel, R. Ionescu, R. Birjega, M. Badea, R. Zavoianu, Journal of Molecular Catalysis A Chemical 352 (2012) 21–30.
[42] P. Mastrorilli, C.F. Nobile, G.P. Suranna, L. Lopez, Tetrahedron 51 (1995) 7943–7950.
[43] G.J. ten Brink, I.W.C.E. Arends, R.A. Sheldon, Chemical Reviews 104 (2004) 4105–4123.
[44] N. Komiya, T. Naota, Y. Oda, S.I. Murahashi, Journal of Molecular Catalysis A Chemical 117 (1997) 21–37.

Please cite this article in press as: K. Leus, et al., Ti-functionalized NH_2-MIL-47: An effective and stable epoxidation catalyst, Catal. Today (2012), http://dx.doi.org/10.1016/j.cattod.2012.09.037